A comment on the use of flushing time, residence time, and age as transport time scales

Abstract—Applications of transport time scales are pervasive in biological, hydrologic, and geochemical studies yet these times scales are not consistently defined and applied with rigor in the literature. We compare three transport time scales (flushing time, age, and residence time) commonly used to measure the retention of water or scalar quantities transported with water. We identify the underlying assumptions associated with each time scale, describe procedures for computing these time scales in idealized cases, and identify pitfalls when real-world systems deviate from these idealizations. We then apply the time scale definitions to a shallow 378 ha tidal lake to illustrate how deviations between real water bodies and the idealized examples can result from: (1) non-steady flow; (2) spatial variability in bathymetry, circulation, and transport time scales; and (3) tides that introduce complexities not accounted for in the idealized cases. These examples illustrate that no single transport time scale is valid for all time periods, locations, and constituents, and no one time scale describes all transport processes. We encourage aquatic scientists to rigorously define the transport time scale when it is applied, identify the underlying assumptions in the application of that concept, and ask if those assumptions are valid in the application of that approach for computing transport time scales in real systems.

In aquatic systems, most of the living biomass and masses of nutrients, contaminants, dissolved gases, and suspended particles are carried in a fluid medium, so it is essential to understand hydrodynamic processes that transport water and its constituents. A first-order description of transport is expressed as "residence time" or "flushing time," which we conceive as measures of water-mass retention within defined boundaries. Aquatic scientists often estimate retention time and compare it to time scales of inputs or biogeochemical processes to calculate mass balances or understand dynamics of populations and chemical properties. Boynton et al. (1995) argue that residence time is such an important attribute that it should be the basis for comparative analyses of ecosystem-scale nutrient budgets.

The classical empirical model of lake eutrophication (Vollenweider 1976) describes algal biomass as a function of phosphorus loading rate scaled by the hydraulic residence time. Since Vollenweider's recognition that the biogeochemical processing of phosphorus varies with residence time, variable water retention or flushing has been used to describe variability of lake thermal stratification (Hamilton and Lewis 1987), isotopic composition (Herczeg and Imboden 1988), alkalinity (Eshleman and Hemond 1988), dissolved organic carbon concentration (Christensen et al. 1996), elemental ratios of heavy metals (Hilton et al. 1995) and nutrients (Hecky et al. 1993), mineralization rates of organic matter (den Heyer and Kalff 1998), and primary production (Jassby et al. 1990). The mechanistic explanation of low plankton abundance in rivers is short residence time relative to population growth rate (Basu and Pick 1996). The occurrence of harmful algal blooms (Bricelj and Lonsdale 1997), distribution of pelagic bacteria (Painchaud et al. 1996), export of copepod life stages (Ohman and Wood 1996), partitioning of primary production between macroalgae and phytoplankton (Valiela et al. 1997), and variability of dissolved nutrient concentrations (Andrews and Müller 1983) in estuaries and other coastal ecosystems are all strongly influenced by residence time.

These examples, all published in *Limnology and Oceanography,* illustrate that applications of transport time scales are pervasive in biological, hydrologic, and geochemical studies. From a survey of these applications and other literature, we identified flushing time, age, and residence time as three fundamentally different concepts of transport time leading to three different approaches for calculating this scale. In some applications (e.g., Hecky et al. 1993; den Heyer and Kalff 1998) the computation of transport time has been done without specification of the underlying concept used. In other cases (e.g., Andrews and Müller 1983; Hilton et al. 1995; Painchaud et al. 1996), the underlying concept and computational steps have been based on an idealized circumstance that is constrained by critical assumptions, but the validation (or even recognition) of those assumptions has not always been considered when applied to a real river, lake, or estuary. Given the central importance of the transport time concept and the varied approaches used, we imagined the usefulness of a comment to reprise the advice of Bolin and Rodhe (1973, p. 58): "To avoid misunderstandings and even erroneous conclusions it is important to introduce precise definitions and to use them with care."

Our goals are to (1) compare three transport time scales commonly used to measure the retention of water or scalar quantities transported with water, (2) identify the underlying assumptions associated with each time scale, (3) describe procedures for computing these time scales in idealized cases, and (4) identify pitfalls when real-world systems deviate from these idealizations. We illustrate how different approaches can yield time scales differing by an order of magnitude, even when applied to the same problem. These differences occur either because a key transport process (e.g., tidal dispersion) is not accounted for in an approach or because the approaches include assumptions that constrain their applicability to either system-level or local-level processes. Furthermore, we explain how the complexities of real aquatic systems—including nonsteady flows, spatial heterogeneity, and oscillatory tidal transports—violate the theory built from idealized circumstances and influence the magnitude of transport times. Our purpose is to stimulate critical thinking in the application of transport time concepts and in the computation of these

time scales where hydrodynamics are more complex than in the idealized cases.

Three transport time scales: The idealized cases—Flushing time: Flushing time (T_f) is a bulk or integrative parameter that describes the general exchange characteristics of a waterbody without identifying the underlying physical processes, the relative importance of those processes, or their spatial distribution. Geyer et al. (2000, p. 191) defined flushing as "the ratio of the mass of a scalar in a reservoir to the rate of renewal of the scalar." T_f can be calculated as the volume of water in a defined (bounded) system (V) divided by the volumetric flow rate (Q) through the system.

$$T_f = \frac{V}{Q} \quad (1)$$

For conservative, miscible quantities associated with the water, flushing can be defined alternatively (Fischer et al. 1979) as

$$T_f = \frac{M}{F} \quad (2)$$

where M is mass of the scalar in the domain and F is flux of the scalar through the domain. Application of this definition requires estimates of both the system volume (or its contained mass) and the exchange rate through the system (flow or mass flux).

Because the quantities V (or M) and Q (or F) often are not known, computation of T_f is sometimes based on the assumption that a waterbody functions as a continuously stirred tank reactor (CSTR), so that flushing time can be estimated from observations of outflow concentration over time. For example, Eshleman and Hemond (1988) assumed a CSTR model to predict alkalinity in a reservoir and compared model results to measured alkalinity at the outflow spillway.

The major assumption for the CSTR model is that any introduction of mass is instantaneously and evenly mixed throughout the domain, so the concentration of a constituent exiting the system is equal to the concentration everywhere inside the CSTR. If we assume that (1) a load of known mass is injected into a CSTR at (time) $t = 0$, resulting in an initial concentration C_0, (2) no further mass is introduced after $t = 0$, and (3) flow and the volume of the CSTR remain constant over time, the concentration inside the CSTR is (Thomann and Mueller 1987)

$$C(t) = C_0 e^{-(Q/V)t} = C_0 e^{-t/T_f} \quad (3)$$

For example, Fig. 1a compares exit concentration calculated by Eq. 3 with experimental data for a CSTR used for blending chemicals into water (Viessman and Hammer 1993). Equation 3 can be rearranged to solve for T_f from a linear regression of time series of measured exit concentrations, yielding the e-folding flushing time as defined by Eq. 4.

$$\ln C(t) = -\left(\frac{1}{T_f}\right)t + \ln C_0 \quad (4)$$

A few subtleties of this approach should be noted. Although "flushing time" implies complete renewal of the sys-
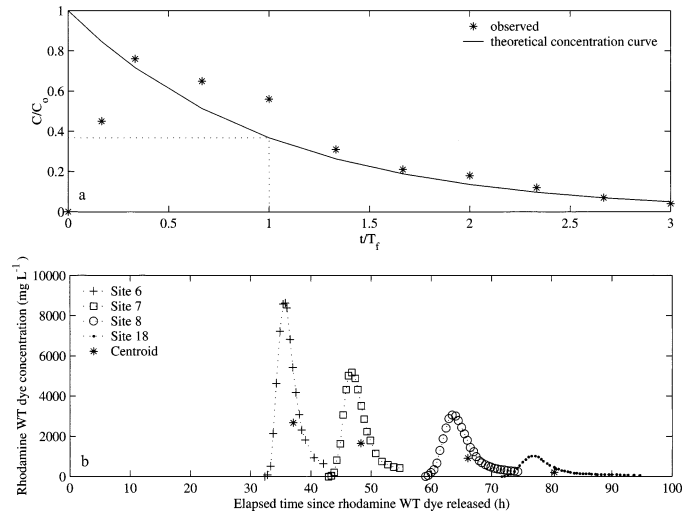

Fig. 1. (a) Theoretical concentration curve for a CSTR based on the analytical solution (Eq. 3) compared to observed effluent concentrations from a completely mixed reactor experiment. (Data are from table 10.1 in Viessman and Hammer [1993] and originally appeared in Marske and Boyle [1973].) The theoretical residence time of the experimental tank was 60 s. (b) Dye release study on the San Joaquin River. Figure re-drawn from Kratzer and Biagtan (1997). Rhodamine WT dye was released 45.9 river km upstream of Site 6 as a slug in the center of the channel. Water was sampled over time at four downstream locations. The distance between Site 6 and Site 18 was 57.1 river km. The centroid value designates the mean age of the dye mass at each station.

tem, the solution to the CSTR model is an exponential curve, so the introduced mass never completely leaves the system and flushing is never complete. The CSTR flushing time only reflects the average amount of time the mass spends in a system. Notice in Fig. 1a that 37% (e^{-1}) of the initial mass still remains in the system at $t = T_f$. Also notice that the calculated mass exits the system immediately, a consequence of the zero-dimensional assumption of instantaneous homogenization of the introduced mass. The experimental results in Fig. 1a were from a chemical processing operation. Even in these ideal circumstances, there is a lag between actual mass introduction and nonzero effluent concentration. In natural systems such as lakes, there is also a time lag between introduction of a scalar quantity and its arrival at the outlet. Textbooks (e.g., Levenspiel 1972) address the problem of how to account for differences between an ideal CSTR and a real stirred tank. Here, it is sufficient to recognize that the "ideal" case of a CSTR does not completely represent real systems.

The tidal prism method is an alternative, classical approach to estimating flushing time in tidal systems when only basin geometry and tidal range information are available. The approach assumes that tides exclusively flush the system (Dyer 1973). Flushing time using this approach is

$$T_f = \frac{VT}{(1 - b)P} \quad (5)$$

The tidal prism (P) is the domain volume between high and low tide marks. This volume is sometimes estimated as the

tidal range (R) multiplied by the surface area at mean sea level. Dividing P by the tidal period (T) converts the prism volume into a flow rate. V is the mean basin volume. Equation 5 is modified by the return flow factor (b), the fraction (0.0–1.0) of effluent water returning to the domain each flood tide. This factor is a function of the fate of the effluent once it leaves the domain and cannot be estimated from basin geometry (Sanford et al. 1992).

Several assumptions form the basis of the tidal prism method. First, the system must be well mixed. Second, river flow must be small compared to tidal flow. Third, the receiving water (water directly outside the domain) must be large enough to dilute the water exiting the basin so that receiving water quality does not change over time and is not materially affected by the effluent (Sanford et al. 1992). Finally, the system should be at steady state with a sinusoidal tide signal.

The tidal prism method tends to underestimate flushing time because the method assumes that the system is well mixed (Dyer 1973; Sanford et al. 1992; Oliveira and Baptista 1997). Luketina (1998) gives an extensive derivation of the tidal prism method and suggests several approaches to improve the results.

Age: Unlike flushing time, age is unique to each water parcel that enters the domain of interest. Zimmerman (1988, p. 76) defines age as "the time [a water parcel] has spent since entering the estuary through one of the boundaries." Inherent to the age time scale is recognition of spatial heterogeneity: particles at different locations within a waterbody have different ages. Consider a pulse dye release study in a nontidal, near-steady-state, one-dimensional river (Kratzer and Biagtan 1997; Fig. 1b). As the pulse of dye travels downstream, dye is observed at different stations at different times. Therefore, the average dye mass age at a downstream location (e.g., Site 18) will be greater than the average dye mass age at an upstream station (e.g., Site 6). In addition, dispersion causes the initial scalar spike to spread. Therefore, at each site some mass arrives having a greater than average age while other mass arrives having a less than average age. In this example, all the dye mass entered the system at the same time. In real systems, mass can enter continuously; therefore, a parcel at a specified location can contain mass with a distribution of ages.

Residence time: Residence time is "the time it takes for any waterparcel of the sample to leave the lagoon through its outlet to the sea" (Dronkers and Zimmerman 1982, p. 108). Residence time is measured from an arbitrary start location within the waterbody. For example, Brooks et al. (1999) quantified the residence time of nutrients (represented as neutrally buoyant particles) released from salmon aquaculture locations in Cobscook Bay to determine whether eutrophication would become a problem between the release location and the bay exit.

Residence time is the complement to age: age is the time required for a parcel to travel from a boundary to a specified location within a waterbody; residence time is how long a parcel, starting from a specified location within a waterbody, will remain in the waterbody before exiting. Age and resi-

dence time depend on the specification of the boundary, the measurement point of interest within the domain, and in tidal systems, the time of release. Unlike the (zero-dimensional) CSTR model, the concepts of residence time and age inherently acknowledge finite transport times through the system.

Deviations between theory and reality: Application to a tidal lake—We illustrate here three major differences between real systems and the idealized examples illustrated above: (1) nonsteady flow; (2) spatial variability in bathymetry, circulation, and transport time scales; and (3) tides that introduce complexities not accounted for in the idealized cases. To illustrate these differences, we apply the time scale definitions described above to Mildred Island (MI), a shallow 378-ha tidal lake in the Sacramento–San Joaquin River Delta (Fig. 2). MI is bounded by a levee with two main openings (the larger in the northeast and the smaller in the south) that provide hydrodynamic connection with adjacent channels. Mean water depth inside MI is a relatively uniform ~5 m, except for a deep (~20 m) area at the northeast entrance. MI is ~1.5 km wide by ~3 km long. Its geometry is irregular, with sharply curved levees creating quiescent side embayments. Bottom friction damps the currents inside MI (maximum tidal velocity ~0.1 m s^{-1}) relative to currents in the deeper neighboring channels (~0.4 m s^{-1}). Flows through the levee breaks are driven by tides and freshwater inputs from the Sacramento and San Joaquin Rivers. Tidal fluctuations in water elevation (tidal range is ~1 m) and currents occur predominantly over the semidiurnal (~12.4-h period) and neap-spring (~14-d period) cycles. This system is characterized by natural and anthropogenic forcings representing a broad range of characteristic frequencies and resulting in the absence of any hydrodynamic steady state.

A series of recent field experiments (Fig. 3) revealed that MI is characterized by substantial spatial and temporal variability in currents and mixing. Drifter studies (http://sfbay.wr.usgs.gov/access/flow/drifterstudies/, pers. comm.; Fig. 3a) show that tidal excursions and dispersion are greater in the north, where the levee opening is wider and deeper than in the south. Lucas et al. (in press) measured sharp north–south gradients in temperature (Fig. 3b), specific (i.e., standardized to 25°C) conductivity (Fig. 3c), chlorophyll *a* (Chl *a,* Fig. 3d), and dissolved oxygen (Fig. 3e), with maxima for all in southeast MI, suggesting longer retention of water, dissolved substances, and particles in the south than in the north. Our interest in quantifying transport time scales in MI was stimulated by the search for a mechanistic understanding of this spatial variability, which is consistent with the notion of spatially variable transport time scales.

To illustrate the concepts of flushing time, age, and residence time for MI, we used Delta TRIM3D, a multidimensional hydrodynamic and scalar transport model. The core of the hydrodynamic model was developed by Casulli and Cattani (1994), and the associated scalar transport routines were incorporated by Gross et al. (1999). The model has been applied to the bathymetry of the Delta and then calibrated and compared against measured stage, flow, and salinity (Monsen 2001). The numerical model is driven at the western boundary with measured tides at Martinez (Fig. 2), and the river boundaries are specified with measured flows
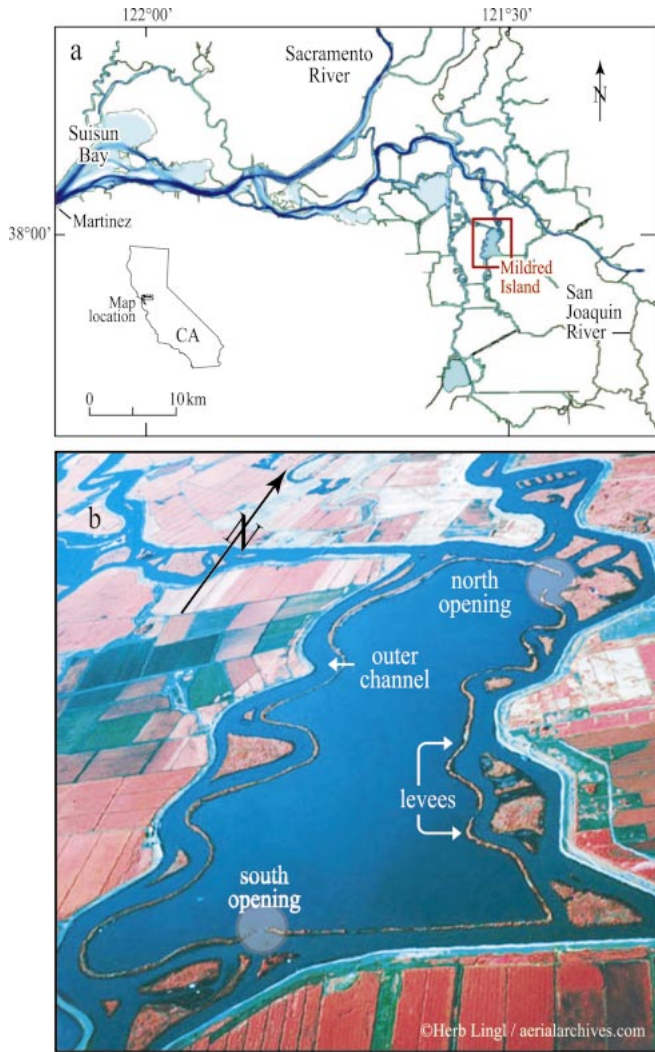
Fig. 2. (a) Map of the Sacramento–San Joaquin Delta. (b) Infrared aerial photograph of Mildred Island. The main levee break is in the northeast corner (upper right, ~18 m deep and ~170 m wide). A secondary break in the south is ~1 m deep and ~50 m wide. Other small breaks (<50 m wide) along the eastern and south sides are too small to be resolved with the numerical model. The interior of Mildred Island is fairly uniform in depth (~5.0 m), except for a deeper region in the northeast corner.
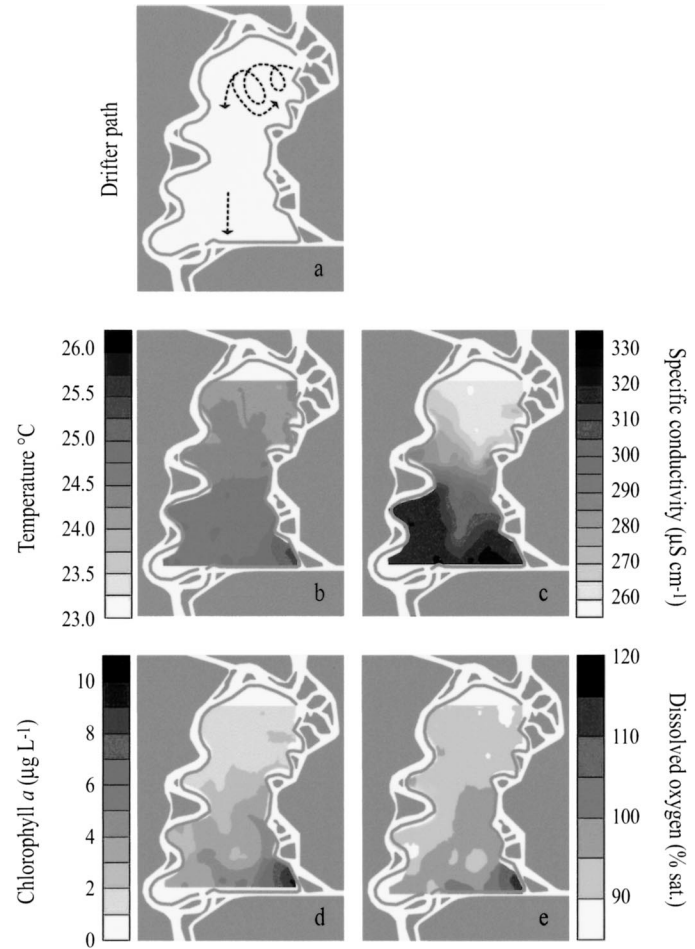

Fig. 3. (a) Mildred Island drifter study, November 1998 (Cuetara and Burau, pers. comm.). Near-surface distributions of (b) water temperature, (c) specific conductivity, (d) Chl *a* concentration, and (e) dissolved oxygen concentration from continuous water quality mapping on 16 June 1999 (Lucas et al. in press).

on the Sacramento and San Joaquin Rivers. Results presented here were calculated using the model in two-dimensional depth-averaged mode, with a grid resolution of 50 m and a 40-s time step. In the following illustrations, the trajectories of neutrally buoyant conservative particles were calculated from the velocity field produced by the hydrodynamic model. The velocity at each particle location was calculated during each time step by linearly interpolating velocities at grid cell walls using the approach of Cheng et al. (1993). We focus on the low-flow conditions of June 1999, a period for which results of drifter experiments and water quality mapping are available for model validation. Each simulation began on 1 June 1999, and transport time scale calculations were initiated on 5 June 1999 to allow for

model "ramp-up" and purging of initial condition information.

Recall that flushing time is an integrative system measure, whereas both residence time and age are local measures (i.e., spatially variable within the domain). Selection of the most appropriate transport time scale depends on the guiding question. If the question involves a comparison of general characteristics between different water systems, a system measure might be appropriate. However, if the question involves the importance of a chemical reaction or biological process in a subembayment of the domain, then a local transport estimate might be necessary. Here we will demonstrate the calculation of both system and local parameters for MI in June 1999.

Flushing time of Mildred Island: Hydrodynamic simulations show that instantaneous flow at the primary (north) MI entrance was strongly influenced by tides (Fig. 4), with flow alternating between a maximum of about +200 m³ s⁻¹ (flood) and a minimum of about −200 m³ s⁻¹ (ebb); however, residual (tidally averaged) flow was two orders of mag-
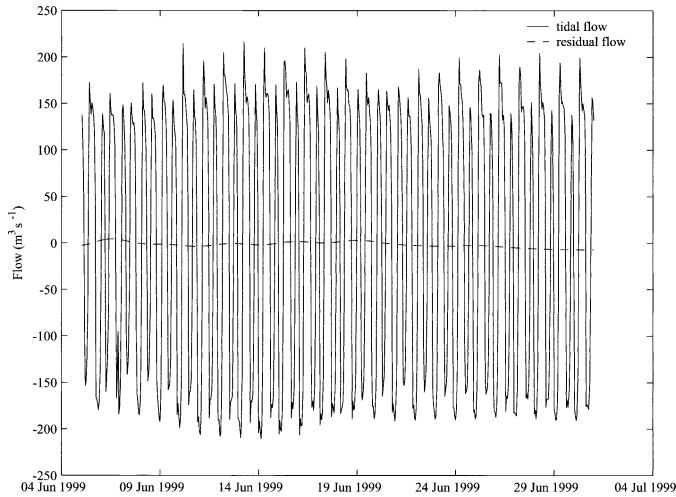
Fig. 4. Tidal and residual flow (flood positive) through Mildred Island north entrance. The residual flow is two orders of magnitude smaller than the tidal flow. This flow was calculated by the Delta TRIM hydrodynamic model for June 1999.
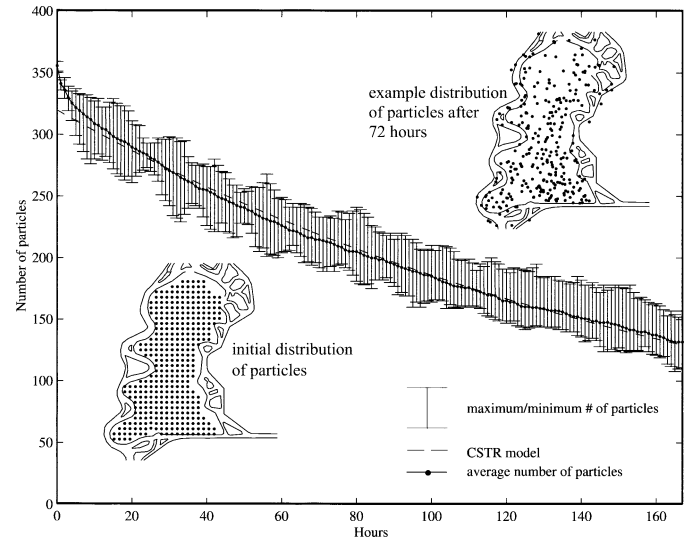

Fig. 5. Estimate of e-folding flushing time for June 1999 using numerical particles and the assumption of a CSTR. The vertical bars indicate the maximum and minimum number of particles present after t hours for all 24 simulations. The solid dark line shows the time series of mean number of particles (averaged over the 24 simulations) retained in MI over the 168-h simulation. Based on the mean particle concentration over time, $T_f = 184.6$ h. (Lower-left inset) Initial particle locations; (upper-right inset) representative particle locations 72 h after release.

nitude smaller, varying slightly over the spring-neap tidal cycle. For this period, the maximum residual flow at the north opening ranged from +4.4 m³ s⁻¹ (into MI) to −7.1 m³ s⁻¹ (out of MI). Using these extreme residual flows (Q) and Eq. 1 to calculate flushing time (where the volume of MI at mean sea level is 1.9×10^7 m³), T_f ranges from 31 to 50 d for these low-flow conditions.

For comparison, we used the same hydrodynamic simulation to calculate the e-folding flushing time, assuming that MI was a CSTR. We initialized the MI model domain with a uniform distribution of 365 particles (Fig. 5) and then calculated the location of each particle over time. During every hour of the simulation period, we recorded the number of particles remaining inside MI. Recognizing that the tidal phase of particle release might influence the calculated flushing time, we conducted 24 different simulations by initializing the same particle field at the beginning of every hour on 5 June 1999 and tracking particles for the subsequent 168 h. Figure 5 shows the summary of these simulations. Using the mean number of particles inside MI at each time step as the concentration time series, we used Eq. 4 to determine the CSTR representation of MI for June 1999. The resulting regression equation ($R^2 = 0.995$) with t in hours is

$$\ln C(t) = -0.00542t + 5.767 \qquad (6)$$

This approach yields a mean flushing time of 7.7 d (184.6 h)—four to six times shorter than the flushing time estimated as V/Q.

The difference between the V/Q estimate and the e-folding estimate of flushing is caused by differences in the basic assumptions inherent in each approach. In the V/Q approach, we assume that the only mechanism of transport is mean advective flux. The particle tracking analysis used in our CSTR approach accounts for additional transport processes such as dispersion (Fischer et al. 1979).

An alternative approach for estimating flushing time that accounts for dispersion is to load the domain of interest with a continuous point source (Dronkers and Zimmerman 1982). Assuming the system eventually reaches equilibrium, the flushing time can be estimated as

$$T_f = \frac{M}{\dot{M}} \qquad (7)$$

where M is the total tracer mass in the system at equilibrium and $\dot{M}$ is a tracer loading rate (mass time⁻¹). Figure 6a shows an application of this approach for MI in June 1999 by specifying a continuous point loading rate $\dot{M} = 100$ kg s⁻¹ at the center of MI. Initially, M within MI increases linearly with time (the period before any mass leaves the domain). After about 3 d, the mass begins to display a tidal signal, and toward the end of the simulation the mass appears to peak and then decline, never sustaining a true steady state. This example illustrates a complication of estimating flushing time in tidal, river-influenced systems where currents and transports vary continuously over multiple frequencies, precluding hydrodynamic steady state. From this numerical experiment, we can estimate the flushing time to be 9.1 d if we estimate M with the peak mass or 8.3 d if we estimate M with the tidally filtered tracer mass at the end of the simulation.

We used this same approach to illustrate the effect of nonsteady flow by applying the same loading rate, $\dot{M}$, but for a period (February 1999) of variable river flow (Fig. 6b). In this case, the loading of tracer began at 1200 h 2 February 1999 during low flow. On about 10 February 1999, a large inflow of water from a winter storm occurred (Fig. 6c) and rapidly diluted the tracer mass. After 18 February 1999, the total mass reached quasi-steady state. Using the tidally fil-
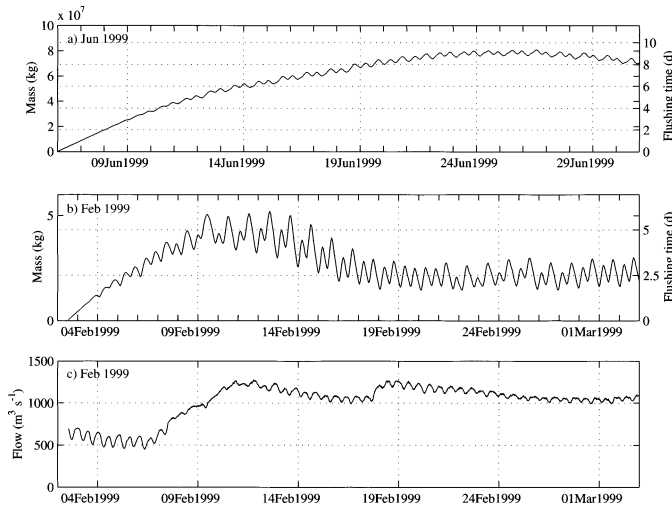
Fig. 6. Time series of total tracer mass in Mildred Island used for the continuous source flushing time estimate for (a) June 1999 and (b) February 1999. Under steady-state conditions, the total mass will plateau to a constant total mass. The flushing time is calculated as the steady-state total mass divided by the rate of loading $\dot{M} = 100$ kg s^{-1}. (c) Observed Sacramento River flow near Locke (RSAC128) for February 1999.

tered total mass at the end of the simulation, the flushing time was ~2.4 d. If the flow had remained constant (~600 m^3 s^{-1}) throughout the simulation, the flushing time would have been greater than 5 d.

In the tidal prism approach for calculating flushing time (Eq. 5), basin geometry (mean volume, surface area), tidal range (R), and the return flow factor (b) are required. Figure 7 shows the range of flushing times expected for MI for four tide ranges (representing the standard range of R in MI over the spring-neap cycle) and all possible return flow factors. For a given tide range, flushing time is sensitive (especially for b > 0.5) to the return flow factor.

Because no guidelines exist for selecting a return flow factor, b, for MI, we will assume here that the flushing times calculated by the CSTR and continuous loading approaches are correct. Using Eq. 5, b = 0.6 for June 1999 (T_f = 8.0 d, R = 0.8 m), and b = −0.1 for February 1999 (T_f = 2.4 d, R = 1.0 m). Therefore, b is not constant for MI, and although the former value of b is plausible, the latter clearly is not. This calculation demonstrates that MI violates several criteria for this approach. First, MI is influenced by river flow. The tidal prism approach worked better for June 1999, a dry period, than for February 1999, a wet period. Second, MI discharges into small channels that are directly affected by exchanges with MI. Third, the tidal range in MI varies over the spring-neap cycle. Finally, hydrologic inputs are unsteady in February 1999 (Fig. 6c). Before applying a time scale approach, consistency between the system and the assumptions of the approach should be checked. This exercise demonstrated that the tidal prism method cannot be appropriately applied to MI.

Age of water parcels in Mildred Island: To illustrate the age concept, we used the particle tracks calculated for the
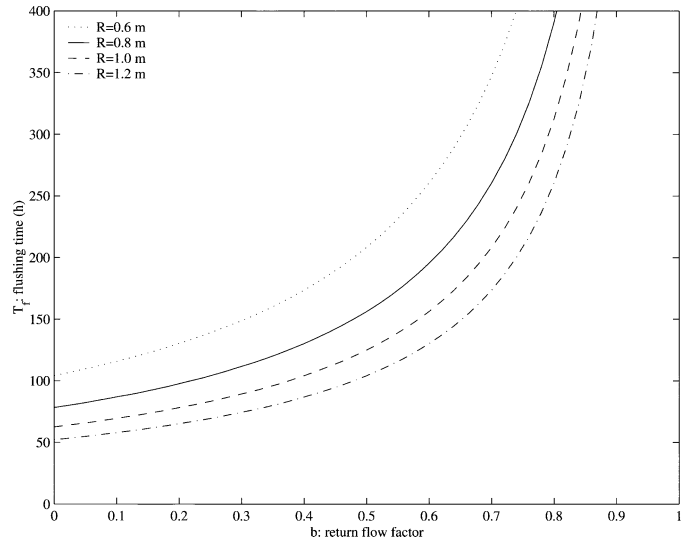

Fig. 7. Possible range of flushing time using the tidal prism approach for Mildred Island for a variable return flow factor (b) and tidal range (R).

June 1999 simulations of MI. Many of the particles initialized inside MI exited the lake on an ebb tide and returned on a later flood tide. We recorded the time when each particle reentered MI and used that entry time as the starting point for calculating that particle's age. We selected 300 × 300 m sampling domains in northern and southern MI (Fig. 8). After each of two periods, T = 84 h and T = 168 h, ages were calculated for all particles in these sampling domains. Note from the results in Fig. 8 that there was a dis-
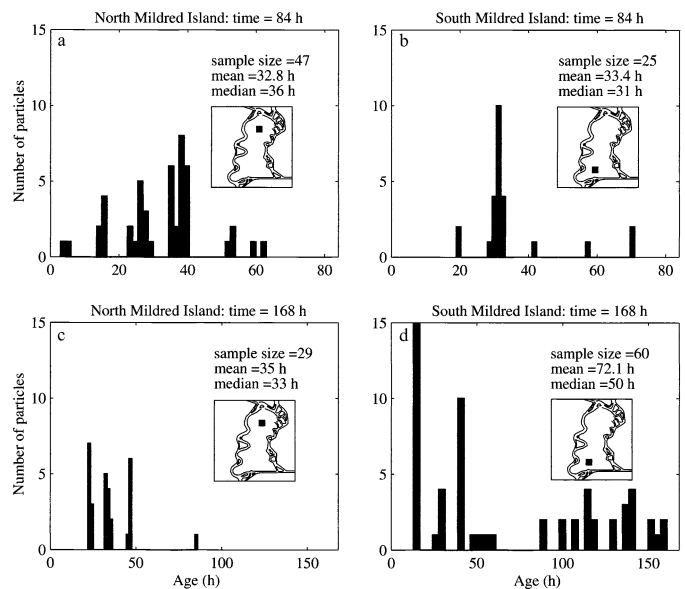

Fig. 8. Numerical particle age distribution for June 1999 within 300- × 300-m sampling domains in (a, c) northern and (b, d) southern Mildred Island. Particles were sampled two times after the simulation began: (a, b) t = 84 h and (c, d) t = 168 h. Transport of particles was calculated by Delta TRIM. Note the change in x-axis scale between the two sampling periods.

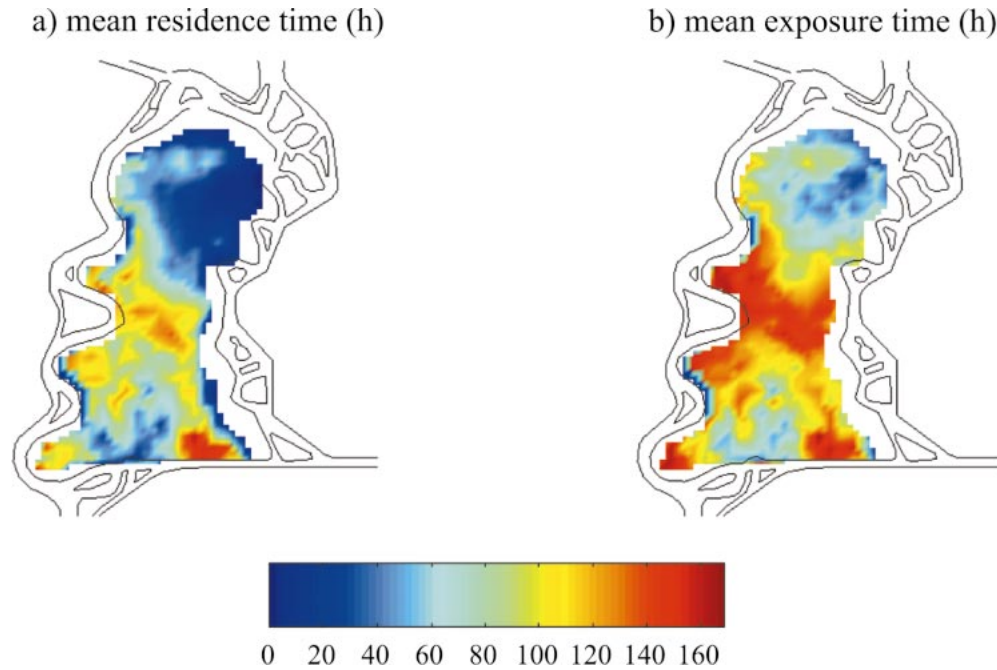## a) mean residence time (h)   b) mean exposure time (h)

Fig. 9. (a) Mean residence time and (b) mean exposure time for June 1999. The mean reflects the average value at each particle release point for 24 different simulations. The maximum time of 168 h reflects the end of the simulation rather than the maximum residence or exposure time. Exposure is the measure of the total time a particle spends inside the boundaries of MI during the simulation, whereas residence time reflects the time the particle stayed in the domain before exiting once.

tribution of particle ages for any sample location and sample period.

These results reveal important lessons about transport and mixing in MI and provide evidence in support of our field-based hypotheses. First, the field data (Fig. 3b–e) suggest that water resided longer in the south than the north. The mean age at the later sampling time in the south (Fig. 8d) is at least twice that in the north (Fig. 8c). The field drifter studies (Fig. 3a) also suggest a more rapid exchange of water with the channels in the north. The mean and median age of particles in the north (Fig. 8a,c) is the same (~33–36 h) for both sample periods, suggesting this region has reached a quasi-steady-state exchange condition with the channel. The south station (Fig. 8b,d) does not reach a quasi-steady-state condition as rapidly. The mean age at the south station approximately doubles between the sampling periods. These results cannot tell us when (or if) the south region reached equilibrium during the simulation period.

Residence time of Mildred Island: Residence time provides a method for quantifying spatial heterogeneity in the distribution of particles (Fig. 5, upper inset) and how long those particles spend in MI before exiting. Recall that residence time is the time required for a water parcel to exit the domain for the first time. Using the particle tracking simulation for MI in June 1999, we recorded the time when individual particles first left the system and from these records created a residence time map. Because MI is a tidal system with time-varying currents, the residence time map will be different if particles are released on different phases of the tide. Therefore, 24 model simulations were executed, with particles released at the beginning of 24 different hours on 5 June 1999. Particle locations were recorded over 168 h. Figure 9a is a map of spatially variable residence time calculated as the mean residence time from all 24 simulations. Note that mean residence time is extremely heterogeneous, ranging from <1 to >168 h depending on location. As would be expected, locations nearer the entrances to MI have shorter residence times than those far from the openings. Notice, for instance, that residence time is long for particles released at the center of MI because travel times for particles in the center of the domain to an exit are longer than for particles initialized near an exit. Long residence times also appear in the subembayment on the southeastern side of MI. Hydrodynamic simulations show that a circulation gyre sets up in this area and there is little exchange between this corner and the rest of MI, resulting in a longer residence time. (Animations of model results illustrating this concept will be available at Ecological Archives Lucas et al. in press; http://www.esapubs.org/archive/archive_A.htm).

Application of the residence time concept to MI illustrates one of the complications in applying idealized transport time scale definitions to tidal systems. Here, we define residence time as the time for a particle to leave MI once and assign values of residence time to the locations of particle release. This definition does not include consideration of oscillating tidal transport of water and scalars into and out of the lake over multiple tide cycles. The total amount of time a particle spends in the domain ("exposure time") might be a more relevant time scale than residence time for some geochem-

ical or biological processes. For example, the long-term net growth of phytoplankton depends on the full range of growth–consumption conditions along tidal trajectories, and these conditions vary along bathymetry gradients (Lucas et al. 1999). Therefore, the growth dynamics of a patch of phytoplankton in a tidal flow could be a strong function of the total amount of time spent in a particular (e.g., high-growth) environment. In Fig. 9b, we see that the exposure time of particles is longer than the residence time in many regions because particles that exit the system can subsequently re-enter MI. Therefore, the influence of MI habitat might be greater on the particle than would be indicated by the formal residence time concept.

Maps depicting spatial variability of residence and exposure times (Fig. 9) provide strong clues about the importance of transport processes in shaping the spatial patterns of non-conservative quantities such as temperature, specific conductivity, Chl *a,* and dissolved oxygen (Fig. 3). The strong north–south gradients of these quantities reflect the gradients of residence time, suggesting that heat, plankton, and dissolved substances accumulate in the southeastern region because of slow tidal mixing, but not in the northeast region where tidal exchanges with the outer channel system are rapid. Integrative time scales, such as flushing time, provide no information about the connections between transport and spatial heterogeneity of these scalars.

In presenting these calculations of flushing time, age, and residence time for MI, our intent was not to compare the calculated values directly but rather to illustrate and compare various approaches used to estimate transport times. Direct comparison of flushing time, a system-level measure, with residence time, a spatially varying local measure, would require statistical averaging to produce a system residence time. Using a similar particle tracking approach as that used here, Oliveira and Baptista (1997) found that, for their case, the average residence time was the same order of magnitude as the globally calculated flushing time when numerical particles were released at a high enough density and statistically averaged. Therefore, results from a flushing time approach, such as the e-folding time shown in Fig. 5, might not be in conflict with those found with the residence time approach. However, as illustrated in Fig. 9, the particle tracking approach provides more information about local processes and gives strong clues about the mechanisms of spatial heterogeneity. This discussion, however, does demonstrate that local biogeochemical rates should be compared to the appropriate local transport time scale rather than a system-level measure of transport, which might not reflect local conditions.

Our purpose is to encourage aquatic scientists (including ourselves) to develop a practice of (1) defining the transport time scale when it is applied, (2) identifying the underlying assumptions in the application of that concept, and (3) asking if those assumptions are valid in the application of that approach for computing transport time scales in real systems.

The examples used in this Comment were selected to show that there is no single transport time scale for a system that is valid for all time periods, locations, and constituents, and that no one time scale describes all transport processes.

By selecting time scales most appropriate for the questions being addressed and explicitly defining the calculation approach, we can develop a practice that adds rigor to our application of transport time scales for revealing mechanisms of spatial and temporal variability in aquatic systems.

Nancy E. Monsen[1]
James E. Cloern
Lisa V. Lucas

U.S. Geological Survey
345 Middlefield Road
MS #496
Menlo Park, California 94025

Stephen G. Monismith

Department of Civil and Environmental Engineering
Stanford University
Stanford, California 94305-4020

References

ANDREWS, J. C. AND H. MÜLLER. 1983. Space–time variability of nutrients in a lagoonal patch reef. Limnol. Oceanogr. **28:** 215–227.

BASU, B. K., AND F. R. PICK. 1996. Factors regulating phytoplankton and zooplankton biomass in temperate rivers. Limnol. Oceanogr. **41:** 1572–1577.

BOLIN, B., AND H. RODHE. 1973. A note on the concepts of age distribution and transit time in natural reservoirs. Tellus **25:** 58–62.

BOYNTON, W. R., J. H. GARBER, R. SUMMERS, AND W. M. KEMP. 1995. Inputs, transformations, and transport of nitrogen and phosphorus in Chesapeake Bay and selected tributaries. Estuaries **18:** 285–314.

BRICELJ, V. M., AND D. J. LONSDALE. 1997. *Aureococcus anophagefferens*: Causes and ecological consequences of brown tides in U.S. mid-Atlantic coastal waters. Limnol. Oceanogr. **42:** 1023–1038.

BROOKS, D. A., M. W. BACA, AND Y.-T. LO. 1999. Tidal circulation and residence time in a macrotidal estuary: Cobscook Bay, Maine. Estuar. Coast. Shelf Sci. **49:** 647–665.

CASULLI, V., AND E. CATTANI. 1994. Stability, accuracy and efficiency of a semi-implicit method for three-dimensional shallow water flow. Comput. Math. Appl. **27:** 99–112.

CHENG, R. T., V. CASULLI, AND J. W. GARTNER. 1993. Tidal, residual, intertidal mudflat (TRIM) model and its applications to San Francisco Bay, California. Estuar. Coast. Shelf Sci. **36:** 235–280.

CHRISTENSEN, D. L., AND OTHERS. 1996. Pelagic responses to

[1] Corresponding author (nemonsen@usgs.gov).

changes in dissolved organic carbon following division of a seepage lake. Limnol. Oceanogr. **41:** 553–559.

DYER, K. R. 1973. Estuaries: A physical introduction. 2nd ed. John Wiley.

DRONKERS, J., AND J. T. F. ZIMMERMAN. 1982. Some principles of mixing in tidal lagoons. Oceanologica acta. Proceedings of the International Symposium on Coastal Lagoons, Bordeaux, France, 9–14 September, 1981, p. 107–117.

ESHLEMAN, K. N., AND H. F. HEMOND. 1988. Alkalinity and major ion budgets for a Massachusetts reservoir and watershed. Limnol. Oceanogr. **33:** 174–185.

FISCHER, H. B., E. J. LIST, R. C. Y. KOH, J. IMBERGER, AND N. H. BROOKS. 1979. Mixing in inland and coastal waters. Academic Press.

GEYER, W. R., J. T. MORRIS, F. G. PAHL, AND D. A. JAY. 2000. Interaction between physical processes and ecosystem structure: A comparative approach, p. 177–206. *In* J. E. Hobbie [ed.], Estuarine science: A synthetic approach to research and practice. Island Press.

GROSS, E. S., J. R. KOSEFF, AND S. G. MONISMITH. 1999. Three-dimensional salinity simulations of South San Francisco Bay. J. Hydraul. Eng. **125:** 1199–1209.

HAMILTON, S. K., AND W. M. LEWIS JR. 1987. Causes of seasonality in the chemistry of a lake on the Orinoco River floodplain, Venezuela. Limnol. Oceanogr. **32:** 1277–1290.

HECKY, R. E., P. CAMPBELL, AND L. L. HENDZEL. 1993. The stoichiometry of carbon, nitrogen, and phosphorus in particulate matter of lakes and oceans. Limnol. Oceanogr. **38:** 709–724.

HERCZEG, A. L. AND D. M. IMBODEN. 1988. Tritium hydrologic studies in four closed-basin lakes in the Great Basin, U.S.A. Limnol. Oceanogr. **33:** 157–173.

DEN HEYER, C., AND J. KALFF. 1998. Organic matter mineralization rates in sediments: A within- and among-lake study. Limnol. Oceanogr. **43:** 695–705.

HILTON, J., E. RIGG, W. DAVISON, J. HAMILTON-TAYLOR, M. KELLY, F. R. LIVENS, AND D. L. SINGLETON. 1995. Modeling and interpreting element ratios in water and sediments: A sensitivity analysis of post-Chernobyl Ru:Cs ratios. Limnol. Oceanogr. **40:** 1302–1309.

JASSBY, A. D., T. M. POWELL, AND C. R. GOLDMAN. 1990. Interannual fluctuations in primary production: Direct physical effects and the trophic cascade at Castle Lake, California. Limnol. Oceanogr. **35:** 1021–1038.

KRATZER, C. R., AND R. N. BIAGTAN. 1997. Determination of traveltimes in the lower San Joaquin River Basin, California, from dye-tracer studies during 1994–1995. U.S. Geological Survey Water-Resources Investigations Report 97-4018.

LEVENSPIEL, O. 1972. Chemical reaction engineering. 2nd ed. Wiley.

LUCAS, L. V., J. R. KOSEFF, S. G. MONISMITH, J. E. CLOERN, AND J. K. THOMPSON. 1999. Processes governing phytoplankton blooms in estuaries. II. The role of horizontal transport. Mar. Ecol. Prog. Ser. **187:** 17–30.

———, J. E. CLOERN, J. K. THOMPSON, AND N. E. MONSEN. In press. Functional variability of shallow tidal habitats in the Sacramento–San Joaquin Delta: Restoration implications. Ecol. Appl.

LUKETINA, D. 1998. Simple tidal prism models revisited. Estuar. Coast. Shelf Sci. **46:** 77–84.

MARSKE, D. M., AND J. D. BOYLE. 1973. Chlorine contact chamber design-a field evaluation. Water and Sewage Works **120:** 70–77.

MONSEN, N. E. 2001. A study of sub-tidal transport in Suisun Bay and the Sacramento–San Joaquin Delta, California. PhD thesis. Stanford Univ.

OHMAN, M. D., AND S. N. WOOD. 1996. Mortality estimation for planktonic copepods: *Pseudocalanus newmani* in a temperate fjord. Limnol. Oceanogr. **41:** 126–135.

OLIVEIRA, A., AND A. M. BAPTISTA. 1997. Diagnostic modeling of residence times in estuaries. Water Resour. Res. **33:** 1935–1946.

PAINCHAUD, J., D. LEFAIVRE, J.-C. THERRIAULT, AND L. LEGENDRE. 1996. Bacterial dynamics in the upper St. Lawrence estuary. Limnol. Oceanogr. **41:** 1610–1618.

SANFORD, L. P., W. C. BOICOURT, AND S. R. RIVES. 1992. Model for estimating tidal flushing of small embayments. J. Waterw. Port Coast. Ocean Eng. **118:** 635–654.

THOMANN, R. V., AND J. A. MUELLER. 1987. Principles of surface water quality modeling and control. HarperCollins.

VALIELA, I., J. MCCLELLAND, J. HAUXWELL, P. J. BEHR, D. HERSH, AND K. FOREMAN. 1997. Macroalgal blooms in shallow estuaries: Controls and ecophysiological and ecosystem consequences. Limnol. Oceanogr. **42:** 1105–1118.

VIESSMAN, JR., W., AND M. J. HAMMER. 1993. Water supply and pollution control. 5th ed. HarperCollins College.

VOLLENWEIDER, R. A. 1976. Advances in defining critical loading levels of phosphorus in lake eutrophication. Mem. Ist. Ital. Idrobiol. **33:** 53–83.

ZIMMERMAN, J. T. F. 1988. Estuarine residence times, p. 75–84. *In* B. Kjerfve [ed.], Hydrodynamics of estuaries. V. 1. CRC Press.